EXTENDED PDF FORMAT
SPONSORED BY
usb
www.usbweb.com

Contribution of Fish to the Marine Inorganic Carbon Cycle

R. W. Wilson, *et al.*

Science **323**, 359 (2009);
DOI: 10.1126/science.1157972

The following resources related to this article are available online at www.sciencemag.org (this information is current as of January 21, 2009):

Updated information and services, including high-resolution figures, can be found in the online version of this article at:
http://www.sciencemag.org/cgi/content/full/323/5912/359

Supporting Online Material can be found at:
http://www.sciencemag.org/cgi/content/full/323/5912/359/DC1

A list of selected additional articles on the Science Web sites **related to this article** can be found at:
http://www.sciencemag.org/cgi/content/full/323/5912/359#related-content

This article **cites 32 articles**, 7 of which can be accessed for free:
http://www.sciencemag.org/cgi/content/full/323/5912/359#otherarticles

This article appears in the following **subject collections**:
Oceanography
http://www.sciencemag.org/cgi/collection/oceans

Information about obtaining **reprints** of this article or about obtaining **permission to reproduce this article** in whole or in part can be found at:
http://www.sciencemag.org/about/permissions.dtl

Downloaded from www.sciencemag.org on January 21, 2009

Science (print ISSN 0036-8075; online ISSN 1095-9203) is published weekly, except the last week in December, by the American Association for the Advancement of Science, 1200 New York Avenue NW, Washington, DC 20005. Copyright 2009 by the American Association for the Advancement of Science; all rights reserved. The title *Science* is a registered trademark of AAAS.

(~350-km radius) partially liquid core. Furthermore, the field that magnetized 76535, which is ~300 million years older than that recorded by all previously studied lunar samples, is from the early epoch when the Moon would have most likely had a convecting core due to enhanced heat flow and a possible cumulate overturn event (*52*). Finally, the NRM in 76535 indicates that minimum paleointensities were of order microteslas, consistent with the theoretical expectations for a lunar core dynamo (*53*). Our data and these considerations suggest that at 4.2 Ga, the Moon possessed a dynamo field, and by implication a convecting metallic core.

References and Notes

1. H. C. Urey, *Geochim. Cosmochim. Acta* **1**, 209 (1951).
2. N. F. Ness, K. W. Behannon, C. S. Scearce, S. C. Cantarano, *J. Geophys. Res.* **72**, 5769 (1967).
3. P. Dyal, C. W. Packer, C. P. Sonett, *Science* **169**, 762 (1970).
4. S. K. Runcorn *et al.*, *Science* **167**, 697 (1970).
5. J. S. Halekas, R. P. Lin, D. L. Mitchell, *Meteorit. Planet. Sci.* **38**, 565 (2003).
6. D. L. Mitchell *et al.*, *Icarus* **194**, 401 (2008).
7. N. Sugiura, Y. M. Wu, D. W. Strangway, G. W. Pearce, L. A. Taylor, *Proc. Lunar Planet. Sci. Conf.* **10**, 2189 (1979).
8. L. J. Srnka, *Proc. Lunar Sci. Conf.* **8**, 785 (1977).
9. D. A. Crawford, P. H. Schultz, *Int. J. Impact Eng.* **23**, 169 (1999).
10. L. L. Hood, N. A. Artemieva, *Icarus* **193**, 485 (2008).
11. R. R. Doell, C. S. Gromme, A. N. Thorpe, F. E. Senftle, *Science* **167**, 695 (1970).
12. S. K. Rucorn, *Nature* **275**, 430 (1978).
13. M. Fuller, S. M. Cisowski, in *Geomagnetism*, vol. 2, J. A. Jacobs, Ed. (Academic Press, New York, 1987), pp. 307–456.
14. K. P. Lawrence, C. L. Johnson, L. Tauxe, J. Gee, *Phys. Earth Planet Int.* 10.1016/j.pepi.2008.05.007 (2008).
15. D. L. Shuster, B. P. Weiss, *Science* **309**, 594 (2005).
16. D. J. Stevenson, *Rep. Prog. Phys.* **46**, 555 (1983).
17. R. Gooley, R. Brett, J. R. Smyth, J. Warner, *Geochim. Cosmochim. Acta* **38**, 1329 (1974).
18. R. F. Dymek, A. L. Albee, A. A. Chodos, *Proc. Lunar Sci. Conf.* **6**, 301 (1975).
19. G. L. Nord, *Proc. Lunar Sci. Conf.* **7**, 1875 (1976).
20. D. E. Wilhelms, "The Geologic History of the Moon" [Professional Paper 1348, U.S. Geological Survey (USGS), Government Printing Office, Washington, DC, 1987].
21. E. W. Wolfe, "The Geologic Investigation of the Taurus-Littrow Valley: Apollo 17 Landing Site" (Professional Paper 1080, Government Printing Office, Washington, DC, 1981).
22. J. C. Huneke, G. J. Wasserburg, *Lunar Sci.* **VI**, 417 (1975).
23. G. W. Lugmair, K. Marti, J. P. Kurtz, N. B. Scheinin, *Proc. Lunar Sci. Conf.* **7**, 2009 (1976).
24. W. R. Premo, M. Tatsumoto, *Proc. Lunar Planet. Sci. Conf.* **22**, 381 (1992).
25. L. Husain, O. A. Schaeffer, *Geophys. Res. Lett.* **2**, 29 (1975).
26. D. D. Bogard, L. E. Nyquist, B. M. Bansal, H. Wiesmann, C.-Y. Shih, *Earth Planet. Sci. Lett.* **26**, 69 (1975).
27. D. A. Papanastassiou, G. J. Wasserburg, *Proc. Lunar Sci. Conf.* **7**, 2035 (1976).
28. G. Ryder, M. D. Norman, R. A. Score, *Proc. Lunar Planet. Sci. Conf.* **11**, 471 (1980).
29. R. M. Bozorth, *Ferromagnetism*. (IEEE Press, New York, 1951), pp. 968.
30. G. W. Pearce, D. W. Strangway, "Apollo 16: Preliminary Science Report" (SP-315, NASA, 1972), chap. 7C, pp. 7–55.
31. J. Gattacceca, P. Rochette, *Earth Planet. Sci. Lett.* **227**, 377 (2004).
32. J. Gattacceca *et al.*, *Phys Earth Planet Inter* **166**, 1 (2008).
33. J. Pohl, A. Eckstaller, *Lunar Planet. Sci.* **12**, 851 (1981).
34. A. Bischoff, D. Stoffler, *Eur. J. Mineral.* **4**, 707 (1992).
35. N. Artemieva, B. Ivanov, *Icarus* **171**, 84 (2004).
36. L. Carporzen, S. A. Gilder, R. J. Hart, *Nature* **435**, 198 (2005).
37. Because some kamacite would have exsolved from taenite during slow-cooling in the deep lunar crust, the HC component is probably a mixture of nonshock TRM and phase-transformation crystallization remanent magnetization (SOM text).
38. I. S. McCallum, J. M. Schwartz, *J. Geophys. Res.* **106**, 27969 (2001).
39. I. S. McCallum *et al.*, *Geochim. Cosmochim. Acta* **70**, 6068 (2006).
40. D. H. Lindsley, D. J. Andersen, *Proc. Lunar Planet. Sci. Conf.* **13**, A887 (1983).
41. C. T. Herzberg, *Lunar Planet. Sci.* **10**, 537 (1979).
42. R. H. Hewins, J. I. Goldstein, *Lunar Planet. Sci.* **6**, 356 (1975).
43. K. Righter, A. J. Campbell, M. Humayun, *Geochim. Cosmochim. Acta* **69**, 3145 (2005).
44. A. Meibom *et al.*, *Science* **288**, 839 (2000).
45. J. R. Smyth, *Proc. Lunar Planet. Sci. Conf.* **17**, E91 (1986).
46. D. Braddy, I. D. Hutcheon, P. B. Price, *Proc. Lunar Sci. Conf.* **6**, 3587 (1975).
47. C. W. Naeser, H. Faul, *J. Geophys. Res.* **74**, 705 (1969).
48. R. A. Ketcham, R. A. Donelick, W. D. Carlson, *Am. Mineral.* **84**, 1235 (1999).
49. R. B. Merrill, M. W. M. McElhinny, *The Magnetic Field of the Earth: Paleomagnetism, the Core, and the Deep Mantle* (Academic Press, San Diego, 1998), p. 531.
50. It is plausible that a small (<10 cm), highly localized, magmatic dike could heat a sample for short timescales; however, such an event would be highly fortuitous, and even more fortuitous to have taken place simultaneously with an impact event.
51. D. W. Collinson, *Surv. Geophys.* **14**, 89 (1993).
52. D. R. Stegman, M. A. Jellinek, S. A. Zatman, J. R. Baumgardner, M. A. Richards, *Nature* **421**, 143 (2003).
53. M. A. Wieczorek *et al.*, *Rev. Mineral. Geochem.* **60**, 221 (2006).
54. J. R. Williams, D. H. Boggs, C. F. Yoder, J. T. Ratcliff, *J. Geophys. Res.* **106**, 27933 (2001).
55. S. Goossens, K. Matsumoto, *Geophys. Res. Lett.* **35**, L02204 (2008).
56. H. Fechtig, S. T. Kalbitzer, in *Potassium Argon Dating*, O. A. Schaeffer, J. Zahringer, Eds. (Springer-Verlag, New York, 1966), pp. 68–107.
57. We thank the Johnson Space Center staff and the Curation and Analysis Planning Team for Extraterrestrial Materials for allocating 76535; V. Fernandes for insights into lunar ^{40}Ar/^{39}Ar geochronology; I. S. McCallum for discussions about thermobarometry; S. Slotznick and S. Pedersen for help with the paleomagnetic analyses; M. Zuber and T. Bosak for suggestions; and K. Willis for administrative help. B.P.W., D.L.S., and I.G.-B. thank the NASA Lunar Advanced Science and Exploration Research Program; B.P.W. thanks the Charles E. Reed Faculty Initiatives Fund for support; and D.L.S. thanks the Ann and Gordon Getty Foundation.

Supporting Online Material
www.sciencemag.org/cgi/content/full/323/5912/356/DC1
SOM Text
Figures S1 to S12
Tables S1 to S3
References

6 October 2008; accepted 3 December 2008
10.1126/science.1166804

Contribution of Fish to the Marine Inorganic Carbon Cycle

R. W. Wilson,[1*] F. J. Millero,[2*] J. R. Taylor,[2] P. J. Walsh,[2,3] V. Christensen,[4] S. Jennings,[5] M. Grosell[2*]

Oceanic production of calcium carbonate is conventionally attributed to marine plankton (coccolithophores and foraminifera). Here we report that marine fish produce precipitated carbonates within their intestines and excrete these at high rates. When combined with estimates of global fish biomass, this suggests that marine fish contribute 3 to 15% of total oceanic carbonate production. Fish carbonates have a higher magnesium content and solubility than traditional sources, yielding faster dissolution with depth. This may explain up to a quarter of the increase in titratable alkalinity within 1000 meters of the ocean surface, a controversial phenomenon that has puzzled oceanographers for decades. We also predict that fish carbonate production may rise in response to future environmental changes in carbon dioxide, and thus become an increasingly important component of the inorganic carbon cycle.

The inorganic half of the marine carbon cycle includes biogenic reaction of seawater calcium (Ca^{2+}) with bicarbonate (HCO_3^-), producing insoluble calcium carbonate ($CaCO_3$) in the process of calcification (*1*):

$$Ca^{2+} + 2HCO_3^- \leftrightarrow CaCO_3 + CO_2 + H_2O$$

The vast majority of oceanic calcification is by planktonic organisms (*2*). Coccolithophores are considered to be the major contributor, but foraminifera are also included in global carbonate budgets (*3*). Upon death, their carbonate "skeletons" are released and rapidly sink to deeper ocean layers. Based on observations and models, estimates of global production of new $CaCO_3$ range from 0.7 to 1.4 Pg $CaCO_3$-C year^{-1} (*4*–*7*) (Fig. 1).

It is less widely known that all marine teleosts (bony fish) produce and excrete carbonate pre-

---

[1]School of Biosciences, University of Exeter, Exeter EX4 4PS, UK. [2]Rosenstiel School of Marine and Atmospheric Science, University of Miami, Miami, FL 33149–1098, USA. [3]University of Ottawa, Ottawa, ON K1N 6N5, Canada. [4]Fisheries Centre, University of British Columbia, Vancouver, BC V6T 1Z4, Canada. [5]Centre for Environment, Fisheries and Aquaculture Science, Lowestoft, and School of Environmental Sciences, University of East Anglia, Norwich NR4 7TJ, UK.

*To whom correspondence should be addressed. E-mail: r.w.wilson@ex.ac.uk (R.W.W.), fmillero@rsmas.miami.edu (F.J.M.), and mgrosell@rsmas.miami.edu (M.G.)

cipitates. Walsh *et al.* (*8*) originally suggested that this might be quantitatively significant on a large scale, an idea not previously considered within a global carbonate budget framework. Carbonate precipitates are excreted by fish via the intestine as a by-product of the osmoregulatory requirement to continuously drink calcium- and magnesium-rich seawater, and they are produced whether or not fish are feeding (*9*). As imbibed seawater passes through the intestine, it is alkalinized (to pH 8.5 to 9.2) along with substantial secretion of HCO_3^- ions, typically reaching 50 to 100 mM in gut fluid (*8*–*11*), well in excess of concentrations in seawater (~2.5 mM). These conditions cause precipitation of imbibed Ca^{2+} (and some Mg^{2+}) ions as insoluble carbonates (*8*–*11*). This process has physiological importance in facilitating water absorption by the gut (*10*), and it reduces calcium absorption, which secondarily protects the kidney by minimizing renal stone formation (*12*). Carbonate precipitates formed in the gut are excreted either within discrete mucus-coated tubes or pellets, or incorporated with feces when fish are feeding (*8*–*10*). The organic mucus-matrix is rapidly degraded in natural seawater, leaving only inorganic crystals of $CaCO_3$ with high magnesium content (Mg:Ca ratio ranging from 10 to 33 mol %) (*8*) (fig. S1).

A striking visual indication of the high rate of carbonate production in marine fish is provided by x-rays of European flounder (*Platichthys flesus*) after acute transfer from fresh water (in which they do not produce carbonates) to seawater (Fig. 2). Accumulations of the precipitates (more x-ray opaque than some of the surrounding bones) can be seen forming inside the intestine within 3 hours of fish initiating drinking after transfer. Excreted carbonates have been collected and titrated to reveal production rates in the temperate European flounder and subtropical Gulf toadfish (*Opsanus beta*) ranging from 18 to 40 μmol C per kg of fish per hour (*8*–*13*). This range is explained by differences in metabolic rate, which are determined by body mass and temperature within a species, as well as by interspecific life-style differences. In aquatic organisms, mass-specific metabolism scales inversely with body size, increasing ~1.6-fold with every 10-fold decrease in body mass, and increases exponentially with temperature typically by 1.83-fold for every 10°C rise (*14*). Thus, smaller fish at higher temperatures produce proportionally more carbonate per unit body mass (fig. S2).

To calculate the teleostean contribution to oceanic carbonate budgets requires knowledge of global marine fish biomass. We used two entirely independent models to describe the size composition and abundance of marine fish across the global oceans, one by using a size-based macroecological approach (*15*) and the other by using Ecopath software (*16*). The fish biomass estimates generated for each size-class and the relevant average local sea temperatures were then combined with individual fish carbonate excretion rates to predict global fish $CaCO_3$ production ranging from 3.2×10^{12} to 8.9×10^{12} mol year^{-1} (0.04 to 0.11 Pg of $CaCO_3$-C year^{-1}). This range accounts for 2.7 to 15.4% of estimates for total global new $CaCO_3$ production in the surface oceans.

Several potentially biasing assumptions are made in these calculations, but we adopted a conservative approach that, if anything, underestimates fish carbonate production. Adopting the more liberal of these realistic assumptions would yield estimates almost three times as high, i.e., 9 to 45% of total global new $CaCO_3$ production (see Supporting Online Material for details of the above calculations and assumptions). Despite this conservatism, our estimate shows that fish are a major but previously unrecognized source of oceanic carbonate and contribute substantially to the marine inorganic carbon cycle (Fig. 1).

An important question following from this discovery is how the nature and fate of piscine carbonates compares with those from traditionally accepted sources. At the higher pressure and colder temperatures of the deep ocean, seawater becomes undersaturated with respect to $CaCO_3$, leading to dissolution as it sinks, in a reversal of reaction 1; thus, the concentration of dissolved HCO_3^- and CO_3^{2-} increases with depth [measured as an increase in the total alkalinity (TA) of seawater]. Pelagic $CaCO_3$ particles from traditional sources are predicted to dissolve once they reach the chemical lysoclines for either calcite (~4300 and 750 m) or aragonite (~1500 and 500 m), respectively, in the North Atlantic and Pacific Oceans (*1*, *17*–*20*). However, contrary to this view, recent carbonate budgets suggest that the majority (50 to 71%) of carbonates exported from surface waters dissolve at much shallower depths (*4*, *5*, *21*). This results in an increase in TA from ~2400 μM to 2480 and 2500 μM at 1000-m depth, in the North Atlantic and Pacific oceans, respectively (*1*) (Fig. 3), a controversial phenomenon that has puzzled oceanographers for decades (*7*).

The causes of $CaCO_3$ dissolution above the lysocline (*7*) are subject to debate and have been attributed to (i) dissolution in zooplankton guts (*22*–*26*); (ii) dissolution in microenvironments where bacterial oxidation of organic matter enhances this process (*27*); and (iii) dissolution of more soluble forms of $CaCO_3$, including pteropods and high-magnesium calcite (*28*, *29*). However, dissolution in copepod guts can account for only a small portion of the increase of TA (*27*). The sharp increase in TA in the Pacific indicates that a more soluble phase may be dissolving (*28*, *29*), such as high-magnesium calcites that are twice as soluble as aragonite (*30*, *31*). We suggest that a large portion of the increasing TA in surface waters is indeed related to the dissolution of high-magnesium calcites produced by fish. Given their high magnesium content (*8*) (fig. S1) and solubility, we predict that dissolution of piscine carbonates will make a major contribution (up to 26%) to the increase in TA in the shallower oceanic depths and helps at least partially explain this currently perplexing observation (*7*) (Fig. 3).

The above estimate is a global average for fish-derived carbonates and does not take into account the potential for regional hot spots of piscine carbonate production (figs. S4 and S5). Indeed, 50% of fish biomass is predicted to occur

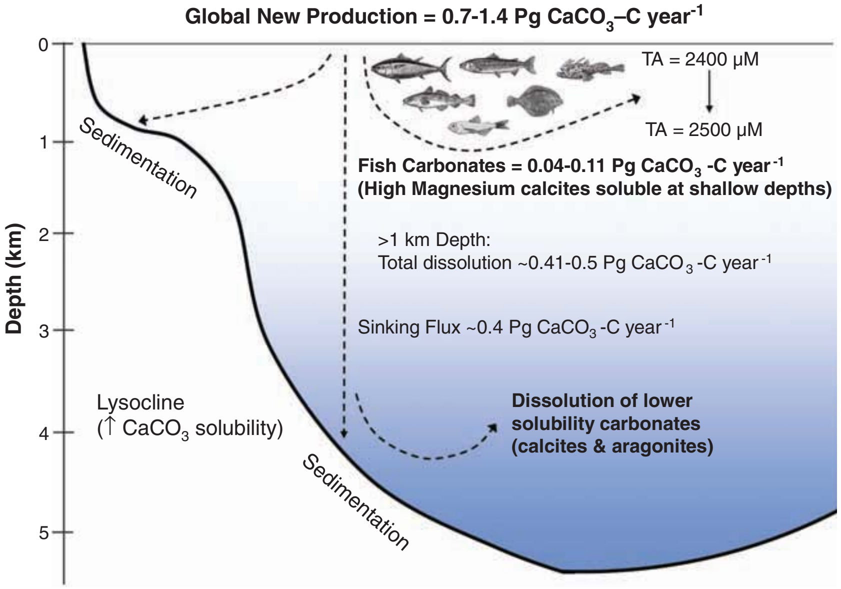

Fig. 1. A modified schematic diagram of ocean $CaCO_3$ budget showing the potential contribution of high-magnesium calcite produced by marine teleost fish. The fish images represent teleosts from a wide range of species and habitats, because all teleosts (but not elasmobranchs) are thought to produce carbonates as part of their osmoregulatory strategy (*8*–*13*). All values except the fish production rate are previously published estimates for total global production or dissolution in the upper ocean (*2*, *5*–*7*).

in only 17% of ocean area (*15*) (fig. S4). Furthermore, such hot spots are largely found over continental shelves and in upwellings where the water is mostly shallow (100 to 200 m deep). This raises the possibility that fish could be the major source of carbonate production in the surface ocean in these areas. Also, dissolution of fish carbonates at such shallow depths may not occur if the carbonates are buried within sediments. Thus, we suggest that the localized high production rates and fate of fish carbonates in some parts of the ocean (and correspondingly low production areas elsewhere) require further investigation. In addition, most carbonates collected in sediment traps cannot be visually identified and accurately assigned to traditional planktonic sources. Intriguingly, some of these collected carbonate particles strongly resemble those found in the intestines of marine fish (fig. S3). The Mg:Ca ratio of fish carbonates (10 to 33 mol %) overlaps with the range for the finest-sized fraction (<37 μm) of magnesian calcite particles collected in sediment traps in the Sargasso Sea (9 to 12 mol %) (*32*). At that time, this magnesian calcite phase of carbonate was assumed to originate from bryozoan skeletons attached to floating Sargassum. It is now tempting to suggest that fish may be the source of this carbonate phase.

So far, we have concentrated on production of carbonates, their excretion, and potential dissolution in the ocean, ignoring a subtle process that further links fish production and distribution to oceanic acid-base chemistry. HCO_3^- ions secreted by intestinal cells into the intestinal lumen of fish are derived largely from metabolic CO_2 reacting with water within intestinal epithelial cells, under the catalytic influence of carbonic anhydrase (*11*). This reaction produces H^+, which is exported into the blood and ultimately excreted into the external seawater via ion-transporting cells in the gills of fish (*12*, *13*). Thus, there is an anatomical separation of, and physical distinction between, the acid and base components of this reaction and its excretory products; i.e., insoluble $CaCO_3$ excreted via the gut, and dissolved H^+ ions excreted via the gills. Furthermore, solid $CaCO_3$ will rapidly sink and only redissolve at depth (raising TA at this point), whereas H^+ ions excreted via the gills will remain in the surface ocean (decreasing TA). Regular vertical migrations of many pelagic fish species, often daily and over several hundred meters, may complicate interpretation of the expected acid-base effects, but the principle is worth noting.

Postindustrial oceanic acidification due to elevated atmospheric CO_2 is now well recognized and is predicted to have major impacts on calcifying organisms (*33*), raising questions about how such future environmental changes may influence piscine global carbonate production. We predict that production of carbonate precipitates by fish will accelerate as a result of both increasing seawater temperatures and CO_2 concentrations. First, metabolic rate increases exponentially with temperature in ectothermic fish, thus increasing metabolic CO_2 production and intestinal carbonate excretion at the individual level (fig. S7). However, for communities, the model of Jennings *et al.* (*15*) suggests that community fish biomass will decrease with temperature (for a given rate of primary production) and that this will offset the accompanying increase in carbonate production owing to temperature effects on individual metabolism. Second, rising ambient levels of dissolved CO_2 will cause a corresponding increase in CO_2 partial pressures in the blood of fish (*34*, *35*). In vitro studies show that increasing blood CO_2 concentrations stimulate intestinal cells to produce more HCO_3^- (*36*), and thus intestinal excretion of precipitated carbonates is predicted to rise with ambient CO_2. This contrasts with the commonly cited view that $CaCO_3$ production rates decrease in calcifying marine plankton and corals as ambient CO_2 increases [(*2*, *33*); but see Supporting Online Material and (*37*)]. The biomineralization mechanisms in these organisms are not well understood (*37*) but are dependent upon the ambient concentrations of CO_3^{2-} or HCO_3^- in seawater, which change with pH as CO_2 concentration increases (*2*). Distinct from this, fish use endogenous CO_2 to produce HCO_3^- ions that rise to very high concentrations within the microenvironment of the gut lumen (typically 50 to 100 mM) (*8*–*11*). Thus, the contribution of fish to marine carbonate production seems likely to increase in the future and become an even more important component of the inorganic carbon cycle.

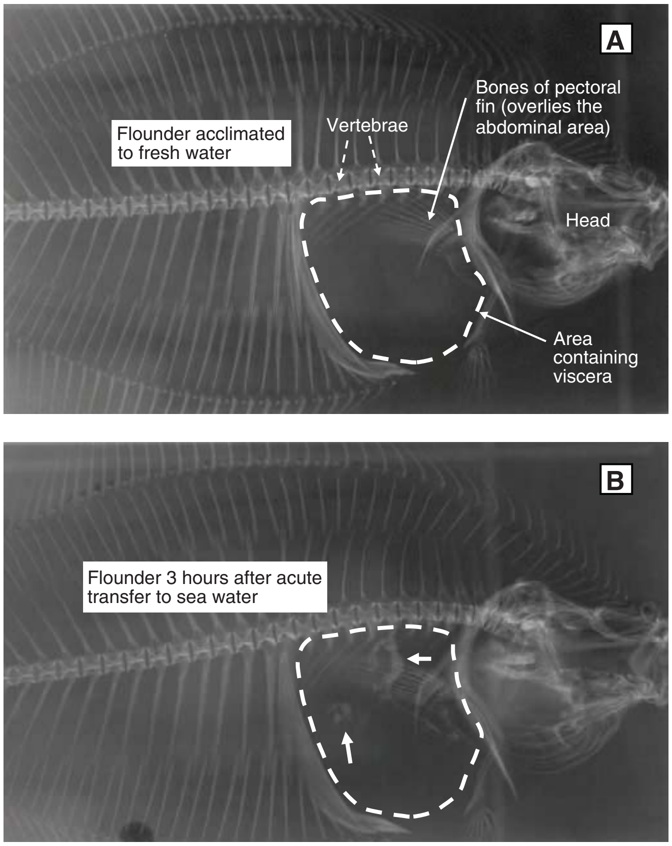

Fig. 2. Digital x-ray photographs of live European flounder (*Platichthys flesus*) showing formation of gut carbonates in unfed fish after transfer from fresh water to seawater. Note the absence of bones (apart from the overlying pectoral fin) over the abdominal area (bounded by dashed line) where the viscera (including intestine) are situated. (**A**) Flounder acclimated to fresh water for 1 week to allow clearance of previously produced carbonates from the intestine. (**B**) X-ray photo taken 3 hours after a freshwater flounder was transferred to seawater. In seawater, the fish rapidly initiates drinking and high rates of intestinal HCO_3^- secretion. This results in the formation of $CaCO_3$ precipitates that form x-ray opaque structures within the intestine (indicated by solid white arrows). X-ray images were taken with Siemens multix-TOP x-ray equipment and a Konica regus computed radiography system.

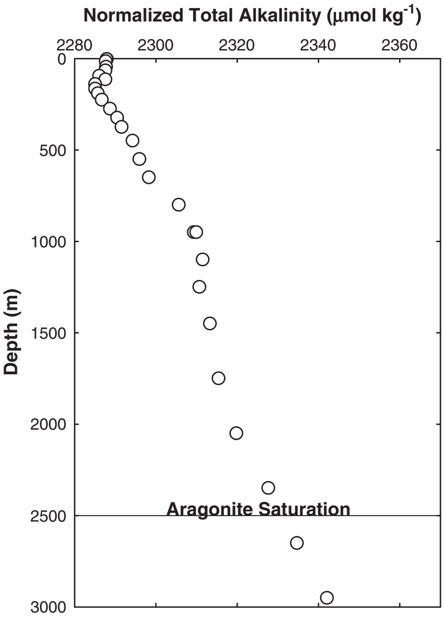

Fig. 3. The normalized total alkalinity of seawater as a function of depth for North Atlantic Waters (30°N and 23°E) (*18*, *20*).

References and Notes

1. F. J. Millero, *Chemical Oceanography* (CRC Press, Boca Raton, FL, ed. 3, 2006).
2. R. A. Feely *et al.*, *Science* **305**, 362 (2004).
3. R. Schiebel, *Global Biogeochem. Cycles* **16**, 1065 (2002).
4. J. D. Milliman, A. W. Droxler, *Geol. Rundsch.* **85**, 496 (1996).
5. K. Lee, *Limnol. Oceanogr.* **46**, 1287 (2001).
6. D. Iglesias-Rodriguez *et al.*, *Eos Trans. AGU* **83**, 365 (2002).
7. J. D. Milliman *et al.*, *Deep Sea Res. Part I Oceanogr. Res. Pap.* **46**, 1653 (1999).
8. P. J. Walsh, P. Blackwelder, K. A. Gill, E. Danulat, T. P. Mommsen, *Limnol. Oceanogr.* **36**, 1227 (1991).
9. R. W. Wilson, K. M. Gilmour, R. P. Henry, C. M. Wood, *J. Exp. Biol.* **199**, 2331 (1996).
10. R. W. Wilson, J. M. Wilson, M. Grosell, *Biochim. Biophys. Acta* **1566**, 182 (2002).
11. M. Grosell, *J. Exp. Biol.* **209**, 2813 (2006).
12. R. W. Wilson, M. Grosell, *Biochim. Biophys. Acta* **1618**, 163 (2003).
13. J. Genz, J. R. Taylor, M. Grosell, *J. Exp. Biol.* **211**, 2327 (2008).
14. A. Clarke, N. M. Johnstone, *J. Anim. Ecol.* **68**, 893 (1999).
15. S. Jennings *et al.*, *Proc. R. Soc. London B. Biol. Sci.* **275**, 1375 10.1098/rspb.2008.0192 (2008).
16. V. Christensen *et al.*, *Models of the World's Large Marine Ecosystems. GEF/LME Global Project Promoting Ecosystem-Based Approaches to Fisheries Conservation and Large Marine Ecosystems* (IOC Technical Series No. **80**, UNESCO, 2008).
17. W. S. Broecker, in *The Fate of Fossil CO_2 in the Oceans*, N. R. Anderson, A. Malahoff, Eds. (Plenum, New York, 1977), p. 207.
18. R. A. Feely *et al.*, *Global Biogeochem. Cycles* **16**, 1144 (2002).
19. C. L. Sabine, R. M. Key, R. A. Feely, D. Greeley, *Global Biogeochem. Cycles* **16**, 1067 (2002).
20. S. Chung *et al.*, *Global Biogeochem. Cycles* **17**, 1093 (2003).
21. C. L. Sabine *et al.*, in *The Global Carbon Cycle: Integrating Humans, Climate, and the Natural World*, C. B. Field, M. R. Raupach, Eds. (Island Press, Washington, DC, 2004), pp. 17–44.
22. T. Takahashi, *Spec. Publ. Cushman Found. Foraminiferal Res.* **13**, 11 (1975).
23. J. K. B. Bishop, J. C. Stepien, P. H. Wiebe, *Prog. Oceanogr.* **17**, 1 (1986).
24. R. P. Harris, *Mar. Biol. (Berlin)* **119**, 431 (1994).
25. P. Van der Wal, R. S. Kempers, M. J. W. Veldhuis, *Mar. Ecol. Prog. Ser.* **126**, 247 (1995).
26. D. W. Pond, R. P. Harris, C. A. Brownlee, *Mar. Biol. (Berlin)* **123**, 75 (1995).
27. H. Jansen, D. A. Wolf-Gladrow, *Mar. Ecol. Prog. Ser.* **221**, 199 (2001).
28. R. H. Byrne, J. G. Acker, P. R. Betzer, R. A. Feely, M. H. Cates, *Nature* **312**, 321 (1984).
29. R. A. Feely *et al.*, *Mar. Chem.* **25**, 227 (1988).
30. J. W. Morse, F. T. Mackenzie, *Geochemistry of Sedimentary Carbonates* (Elsevier, New York, 1990).
31. J. W. Morse, D. K. Gledhill, F. J. Millero, *Geochim. Cosmochim. Acta* **67**, 2819 (2003).
32. V. J. Fabry, W. G. Deuser, *Deep-Sea Res.* **38**, 713 (1991).
33. J. C. Orr *et al.*, *Nature* **437**, 681 (2005).
34. H. O. Pörtner, M. Langenbuch, A. Reipschläger, *J. Oceanogr.* **60**, 705 (2004).
35. B. A. Seibel, P. J. Walsh, *Science* **294**, 319 (2001).
36. M. Grosell *et al.*, *Am. J. Physiol. Regul. Integr. Comp. Physiol.* **288**, R936 (2005).
37. V. J. Fabry, *Science* **320**, 1020 (2008).

38. R.W.W. acknowledges support from the UK Biotechnology and Biological Sciences Research Council (awards BB/D005108/1, BB/F009364/1, and ISIS 1766) and The Royal Society (award RSRG 24241). F.J.M. acknowledges the Oceanographic Section of the U.S. National Science Foundation (NSF). P.J.W. is supported by the Natural Sciences and Engineering Research Council (NSERC) of Canada and the Canada Research Chair program. V.C. acknowledges support from NSERC, the Global Environment Facility's UNEP/UNESCO/IOC (Intergovernmental Oceanographic Commission) LME (Large Marine Ecosystem) activities, and from the Sea Around Us Project, initiated and funded by The Pew Charitable Trusts. S.J. thanks the European Commission and the UK Department of Environment, Food, and Rural Affairs for funding support, and A. Clarke (British Antarctic Survey, Cambridge) for providing a compilation of fish oxygen consumption data. M.G. and S.J. are supported by the NSF (awards 0416440, 0714024, and 0743903). We also thank referees for their insightful comments; K. Knapp (School of Physics, University of Exeter) for the fish x-ray images (Fig. 2); R. Walton (University of Warwick, UK) for the powder x-ray diffraction analysis (fig. S1); H. Stoll (Department of Geoscience, Williams College, Williamstown, MA) and A. Pritchard (University of Exeter, Biosciences) for the scanning electron micrographs of sediment trap samples and fish carbonates, respectively (fig. S3); R. Forster (Centre for Environment, Fisheries and Aquaculture Science, Lowestoft) for plotting fig. S4; FishBase (www.fishbase.org) for providing fish species' information; J. Whittamore for preparation of flounder for x-ray imaging; J. Corcoran and C. Cooper for the sheepshead minnow experiments in the Supporting Online Material; and R. van Aerle for assistance with graphical illustrations.

Supporting Online Material
www.sciencemag.org/cgi/content/full/323/5912/359/DC1
Materials and Methods
SOM Text
Figs. S1 to S6
Tables S1 and S2

18 March 2008; accepted 16 June 2008
10.1126/science.1157972

Morphogenesis of Self-Assembled Nanocrystalline Materials of Barium Carbonate and Silica

Juan Manuel García-Ruiz,[1] Emilio Melero-García,[1] Stephen T. Hyde[2]

The precipitation of barium or strontium carbonates in alkaline silica-rich environments leads to crystalline aggregates that have been named silica/carbonate biomorphs because their morphology resembles that of primitive organisms. These aggregates are self-assembled materials of purely inorganic origin, with an amorphous phase of silica intimately intertwined with a carbonate nanocrystalline phase. We propose a mechanism that explains all the morphologies described for biomorphs. Chemically coupled coprecipitation of carbonate and silica leads to fibrillation of the growing front and to laminar structures that experience curling at their growing rim. These curls propagate in a surflike way along the rim of the laminae. We show that all observed morphologies with smoothly varying positive or negative Gaussian curvatures can be explained by the combined growth of counterpropagating curls and growing laminae.

The theoretical morphology of classical crystals is well accommodated within conventional crystal growth theory, where the development of various crystal faces is accounted for by the relative crystallographic surface energies at the atomic scale, and the overall symmetry is imposed by the atomic-scale packing. The relation between nonequilibrium crystal shapes and their physical and chemical growth conditions is also part of the general picture (*1*). In contrast, despite numerous observations over the years (*2*) that life is able to make precise, smooth, differentiable shapes made of polycrystalline minerals (shells, teeth, bones, etc.), we have a limited understanding of the morphogenetical mechanisms leading to the formation of these fascinating architectures. The laboratory synthesis of actual self-assembled structures mimicking the ability of life to create sinuous noncrystallographic morphologies with crystalline materials is still a challenge. Among the few examples of synthetic self-organized nanocrystalline materials known to display a wealth of morphologies comparable to that of biominerals are silica/carbonate biomorphs (*3*–*5*). Biomorphs, like biominerals, exhibit nanoscale atomic ordering but lack long-range positional order. As a consequence, no characteristic faces or edges are expressed; rather, they are bounded by smoothly curved surfaces. Thus biomorphs, whose morphogenetic mechanism has remained unknown (*5*–*7*), display a zoo of curvilinear morphologies, often indistinguishable from the forms of biomaterials found in vivo.

Silica/barium carbonate biomorphs can be grown routinely by mixing barium chloride solutions with silica solutions and gels within a pH range from 8.5 to 11, at atmospheric pressure and temperature (*8*). Under alkaline conditions, carbonate from dissolved atmospheric CO_2 reacts with Ba^{2+} to precipitate crystalline barium carbonate (witherite) in the form of pseudohexagonal prismatic crystals tapered by bipyramidal faces (*9*). However, it has been shown (*3*–*7*, *10*, *11*) that when barium carbonate crystallizes from silica-rich solutions or from silica gels, it forms polycrystalline aggregates displaying a variety of

---

[1] Laboratorio de Estudios Cristalográficos, Instituto Andaluz de Ciencias de la Tierra, Consejo Superior de Investígaciones Cientificas–Universidad de Granada, Avenida del Conocimiento, Parque Tecnológico, Ciencias de la Salud, 18100 Armilla, Spain. [2] Department of Applied Mathematics, Research School of Physical Sciences, Australian National University, Canberra, Australian Capital Territory 0200, Australia.